

C.-W. CHEN^{1,2}
C.-H. LIN^{1,2}
H.-P. CHIANG^{1,2,✉}
Y.-C. LIU³
P.T. LEUNG^{4,✉}
W.S. TSE⁵

Temperature dependence of the sensitivity of a long-range surface plasmon optical sensor

¹ Institute of Optoelectronic Sciences, National Taiwan Ocean University, Keelung 202, Taiwan, R.O.C.

² Institute of Physics, Academia Sinica, Taipei, Taiwan, R.O.C.

³ Department of Food Science, National Taiwan Ocean University, Keelung, Taiwan, R.O.C.

⁴ Department of Physics, Portland State University, P.O. Box 751, Portland, OR 97207-0751, USA

⁵ Division of Natural Science, Ming Hsin University of Science and Technology, Hsinchu, Taiwan, R.O.C.

Received: 15 January 2007 / Accepted: 2 May 2007
Published online: 21 June 2007 • © Springer-Verlag 2007

ABSTRACT The temperature dependence of the sensitivity of an optical sensor based on long-range surface plasmon resonance (LRSPR) is studied via theoretical modeling. Both the ‘angular interrogation’ and the ‘wavelength interrogation’ modes of operation are studied. In addition, the variation of the full width at half maximum of the LRSPR ‘reflectance dip’ is also studied as a function of temperature, which ultimately determines the temperature dependence of the sensitivity of the sensor when the reflectance is monitored at a fixed incident angle (‘reflectance interrogation’). It is found that while most of the time only the ‘reflectance interrogation’ mode leads to improved sensitivity for the LRSPR sensor compared to a conventional SPR sensor, the temperature stability of the operation of the LRSPR sensor is generally higher than (or at least comparable to) that of the SPR sensor.

PACS 73.20.Mf; 07.07.Df

1 Introduction

It has been well established since the 1980s that efficient optical sensing can be achieved via the excitation of the collective oscillation of the free electrons (known as surface plasmons) at a metal–dielectric interface [1]. This is usually done through attenuated total reflection via the Kretschmann geometry [2], which was first introduced in the early 1970s. Sensitivity of these sensors based on surface plasmon resonance (SPR) can be very high and can comfortably reach picomolar detection of medium–heavy biomolecules such as, for example, in a biosensor application [1].

Then, in 1981, Sarid [3] introduced a mechanism based on the cross coupling between the two SPRs across a metal film of very small thickness (\sim tens of nanometers), leading to the generation of long-range surface plasmons (LRSP) and short-range surface plasmons (SRSP), respectively. The LRSP turn out to be ‘antibonding modes’ which yield an extremely sharp optical reflectance spectrum, due to the decrease in the loss of the fields in the metal. This opens up the possibility to further

increase the sensitivity of a SPR sensor via the excitation of the LRSP. Indeed, Sarid’s mechanism was subsequently verified experimentally [4], and application of it to achieve highly sensitive sensing was also explored [5].

Moreover, it has been known from the very beginning that many physical and chemical factors will affect the ultimate sensitivity of these SPR/LRSPR sensors. One significant factor is the temperature of the sensing environment. In fact, with appropriate calibration, optical sensing of temperatures can be achieved using these SPR sensors [6]. On the other hand, if other sensing parameters (e.g. sample concentration) are being studied, then the effect on the sensing outcome due to the variation of temperature in the environment must be well monitored and controlled.

In a previous investigation [7], we have explored the temperature effects on a conventional Kretschmann SPR sensor via a simple theoretical model. In particular, it was discovered that the ‘angular interrogation’ mode of operation in which the reflectance dip angle is monitored as a function of the analyte concentration has the highest temperature stability in general. In the present work, we will extend our model to study the temperature effects on the corresponding sensitivities of a LRSPR sensor.

2 Theoretical model

We have in mind a LRSPR biosensor in the form of the Sarid geometry [3] as depicted in Fig. 1 by a four-layer system. Layer 3 is a metal (Ag) film of variable thickness sandwiched between a dielectric layer (2) and the sample (analyte). Symmetric (asymmetric) LRSP can be generated when the refractive indices of the dielectric and the analyte match (mismatch) for appropriate thickness for the dielectric and metal layers, respectively. Here we shall assume a symmetric case with (2) being a layer of polymer (Cytop) of thickness 1180 nm and index matching closely to that of water (analyte) – a system recently fabricated by Corn and collaborators for a successful demonstration of the operation of a LRSPR biosensor [8]. Figure 2 shows some typical results for the long- and short-range SPR reflectance dip as a function of incident angle at conditions as specified for the system in Fig. 1. A similar spectrum can be obtained when the re-

✉ Fax: 886-2-24634360, E-mail: hpchiang@mail.ntou.edu.tw

✉ E-mail: hopl@pdx.edu

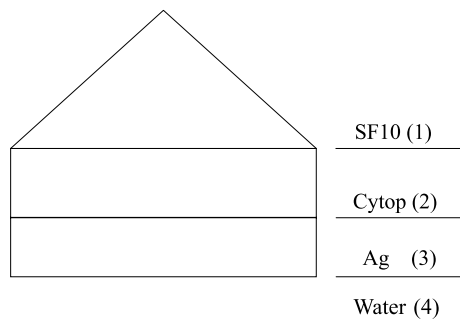


FIGURE 1 Sarid geometry for a LRSR sensor. The four layers are: SF10 ($n_p = 1.711$)/Cytop 1180 nm ($n = 1.336$)/Ag 30–50 nm/water (n_a)

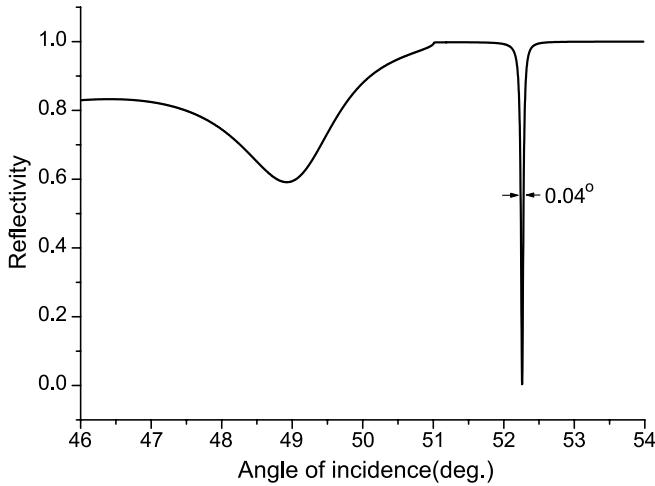


FIGURE 2 Typical angular reflectance curve illustrating the LRSR and the SRSR modes for the geometry in Fig. 1 with incident wavelength 670 nm, Ag thickness 30 nm, $n_a = 1.33$, and temperature 300 K

flectance is plotted as a function of wavelength at a fixed angle of incidence.

A LRSR biosensor monitors the change of the LRSR reflectance dip (the sharper one of the two) as the sample analyte is introduced into the sensor. Among many monitoring schemes, three modes of operation commonly adopted are (i) the ‘angular interrogation’ mode in which the dip angle (θ_m) is monitored as a function of the analyte concentration (n_a); (ii) the ‘wavelength interrogation’ mode in which the dip wavelength (λ_m) is monitored; and (iii) the ‘reflectance interrogation’ mode in which the change in the reflected light intensity is monitored at a fixed angle close to the dip angle. The sensitivities for each of the three modes can be defined as $S_\theta = d\theta_m/dn_a$, $S_\lambda = d\lambda_m/dn_a$, and $S_R = dR/dn_a \propto \Delta\theta$, where $\Delta\theta$ is defined as the full width at half maximum (FWHM) of the LRSR angular reflectance curve. In principle, all these three sensitivities can be calculated from the Fresnel equations as in the case for the ordinary SPR (Kretschmann geometry) sensor [7, 9]. But, since the analytic expressions turn out to be extremely complicated and messy for the LRSR sensor, here we shall resort to a numerical investigation of these quantities as a function of environmental temperatures.

The temperature dependence of these sensitivities arises mainly from the change in optical properties of the metal (Ag) film as the sensor temperature increases. Here we briefly recapitulate a previous model we established to describe these

changes [7, 10]. To begin, we model the dielectric response of the Ag film using the Drude model:

$$\hat{\epsilon}_3 = 1 - \frac{\omega_p^2}{\omega(\omega + i\omega_c)}, \quad (1)$$

where ω_c is the collision frequency and ω_p the plasma frequency given by

$$\omega_p = \sqrt{\frac{4\pi Ne^2}{m^*}}, \quad (2)$$

with N and m^* the density and effective mass of the electrons, respectively. Hence, assuming that the variation of m^* with T can be ignored [7], ω_p depends on T via volumetric effects as follows:

$$\omega_p = \omega_{p0}[1 + \gamma(T - T_0)]^{-1/2}, \quad (3)$$

where γ is the expansion coefficient of the metal and T_0 is a reference temperature taken to be the room temperature. The collision frequency will have contributions from both phonon–electron and electron–electron scattering:

$$\omega_c = \omega_{cp} + \omega_{ce}, \quad (4)$$

and can be modeled using the various scattering models in the literature. We thus obtain [10]

$$\omega_{cp}(T) = \omega_0 \left[\frac{2}{5} + 4 \left(\frac{T}{\theta} \right)^5 \int_0^{\theta/T} \frac{z^4 dz}{e^z - 1} \right], \quad (5)$$

where θ is the Debye temperature and ω_0 is a constant to be determined from the static limit of the above expression together with the knowledge of the d.c. conductivity [10]. In addition, we have [10]

$$\omega_{ce}(T) = \frac{1}{12} \pi^3 \frac{\Gamma \Delta}{\hbar E_F} [(k_B T)^2 + (\hbar\omega/2\pi)^2], \quad (6)$$

where Γ and Δ are defined in [10]. Thus, (1)–(6) provide a model for the temperature dependence of $\hat{\epsilon}_3 = \sqrt{\epsilon_3}$, which when used in the Fresnel equations will lead to temperature-dependent sensitivities for the LRSR sensor.

3 Numerical results and discussion

Figure 3 shows the angular reflectance spectrum of the LRSR dip for several temperatures as computed from our model above. It is seen that the dip slightly shifts towards larger resonance angles as the temperature increases. A similar effect was also observed (not shown) for the resonance wavelength in the spectral reflectance spectrum. We have further analyzed numerically the sensitivities S_θ and S_λ as defined above for a range of analyte refractive indices from 1.332 to 1.338. For an incident wavelength of 670 nm, we have obtained $S_\theta = 31.2^\circ/\text{refractive index units (RIU)}$ and, for θ fixed at 52.22° , $S_\lambda = 9250 \text{ nm}/\text{RIU}$. Both these values are obtained at room temperature ($T = 300 \text{ K}$) and are not noted to be higher than the corresponding ones for a conven-

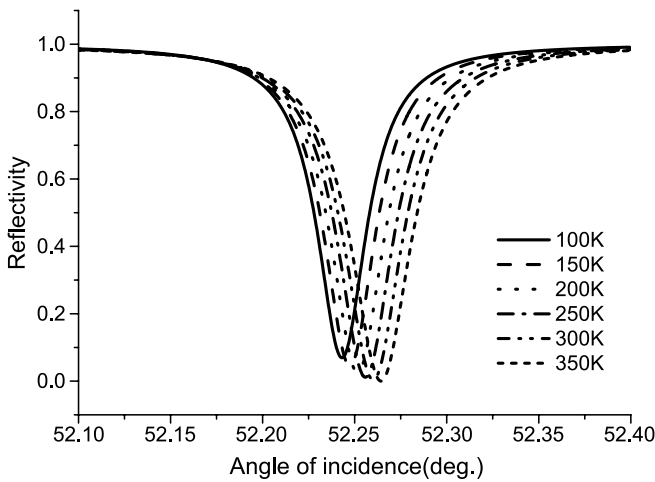


FIGURE 3 Example showing the temperature dependence of the LRSPP reflectance curve in Fig. 2

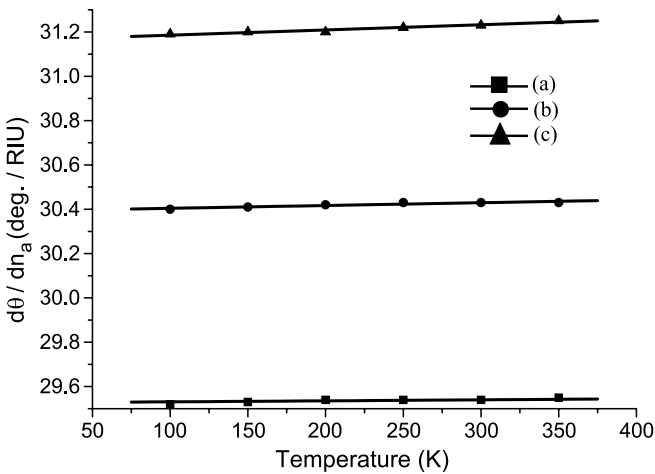


FIGURE 4 Sensitivity in the angular interrogation mode as a function of temperature at different incident wavelengths and Ag film thickness: (a) incident wavelength 670 nm, Ag thickness 30 nm, (b) incident wavelength 750 nm, Ag thickness 40 nm, (c) incident wavelength 830 nm, Ag thickness 50 nm

tional SPR sensor with the same thickness for the silver film of 50 nm. This is in contrast to a previous report [11] in which an appreciable increase of S_λ was observed for a LRSPP sensor using a gold film of thickness varying from about 20 to 40 nm.

Figure 4 shows the results for S_θ as a function of temperature for several different incident wavelengths up to values close to the boiling point of water. A slope of the order of 10^{-4} degree/RIU/K is obtained, which verifies the relative stability of the sensitivity of a LRSPP sensor against variation of temperature. This is similar to the case for an ordinary SPR sensor [7]. Figure 5 shows the corresponding temperature effects on S_λ for sensors with an Ag film of different thickness. A rate of the order of 10^{-1} nm/RIU/K can be obtained by linearly fitting the data, which implies again a relatively stable S_λ against temperature change for the LRSPP sensor. This is somewhat in contrast to the ordinary SPR sensor, in which a large decrease of S_λ can occur as the temperature rises when the dip occurs at long wavelengths (e.g. \sim infrared or far-infrared range) [7].

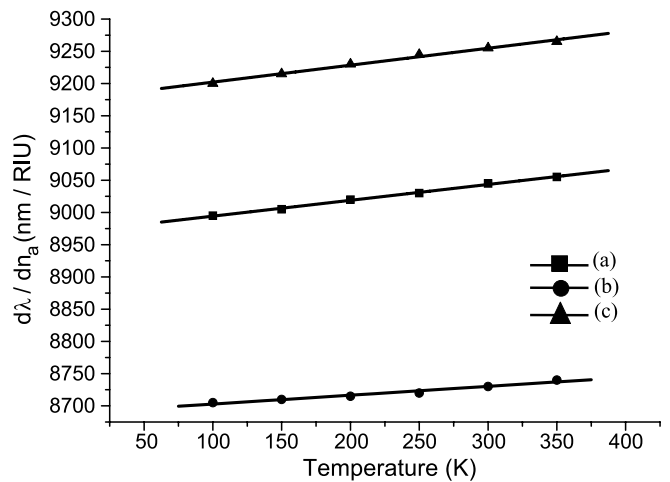


FIGURE 5 Sensitivity in the wavelength interrogation mode as a function of temperature at different incident angles and Ag film thickness: (a) incident angle 52.22°, Ag thickness 30 nm, (b) incident angle 52.4°, Ag thickness 40 nm, (c) incident angle 52.45°, Ag thickness 50 nm

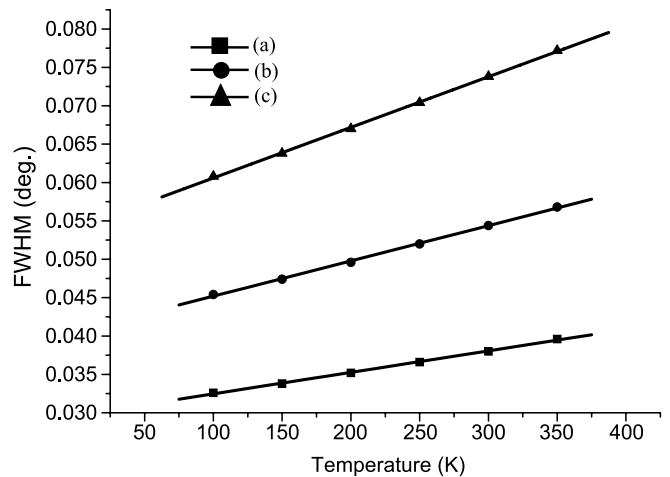


FIGURE 6 Variation of the FWHM of a LRSPP curve with temperature at different wavelengths and metal film thickness: (a) incident wavelength 670 nm, Ag thickness 30 nm, (b) incident wavelength 750 nm, Ag thickness 40 nm, (c) incident wavelength 830 nm, Ag thickness 50 nm. Analyte index is fixed at $n_a = 1.33$

We have also investigated the dependence of the FWHM of the LRSPP reflectance dip as a function of temperature. It has been reported recently that by employing the relatively small values of these sharp dip curves, the LRSPP sensor can have significantly greater sensitivity compared to that of an ordinary SPR sensor [5, 8]. Here we also obtain values for the FWHM for the LRSPP sensor relatively smaller than the corresponding ones for a SPR sensor in general, implying greater sensitivity for S_R . Furthermore, we have studied the temperature dependence of these FWHM values at different wavelengths and Ag film thickness for the LRSPP sensor. The results shown in Fig. 6 lead to a variation of $\Delta\theta$ of the order of 10^{-5} degree/K, which implies again high temperature stability for the reflectance interrogation sensing mode used in a LRSPP sensor. This is again in contrast to the previously studied SPR sensor where a relatively large drop of the sensitivity in this mode was observed as the temperature increases [7].

4 Conclusion

In this work, we have adopted a previously established model for the temperature variation of the surface plasmon resonance of silver to study numerically the stability of the various sensitivities of a LRSPP sensor against temperature changes. It is found that while the angular and wavelength interrogation modes do not necessarily have larger sensitivity compared to those for an ordinary SPR sensor, the reflectance monitoring mode in general yields somewhat higher sensitivity. In addition, the temperature stabilities of all these three modes are found to be better than or comparable to those of the SPR sensor. Further comparison of the operation of these two sensors in terms of the variation of the many other key parameters will be significant for an ultimate design of a more sensitive and stable optical sensor based on surface plasmon resonance.

ACKNOWLEDGEMENTS H.-P. Chiang acknowledges financial support from the Center of Nanostorage Research, National Taiwan University, under Grant No. MOEA#95-EC-17-A-08-S1-0006, the National

Science Council of R.O.C. under Grant Nos. NSC 95-2112-M-019-002 and NSC 95-2120-M-019-001, and the Center for Marine Bioscience and Biotechnology, National Taiwan Ocean University, under Grant Nos. NTOU-AF94-05-04-01-01 and NTOU-AF94-05-04-01-02. P.T. Leung acknowledges a research grant from Intel Corporation.

REFERENCES

- 1 See, e.g., the review article by J. Homola, S.S. Yee, G. Gauglitz, *Sens. Actuators B* **54**, 3 (1999)
- 2 H. Raether, *Surface Plasmons on Smooth and Rough Surfaces and on Gratings* (Springer, Berlin, 1988)
- 3 D. Sarid, *Phys. Rev. Lett.* **47**, 1927 (1981)
- 4 J.C. Quail, J.G. Rako, H.J. Simon, *Opt. Lett.* **8**, 377 (1983)
- 5 K. Matsubara, S. Kawata, S. Minami, *Opt. Lett.* **15**, 75 (1990)
- 6 S. Heminghaus, P. Liederer, *Appl. Phys. Lett.* **58**, 352 (1991)
- 7 H.-P. Chiang, Y.C. Wang, P.T. Leung, W.S. Tse, *Opt. Commun.* **188**, 283 (2001)
- 8 A.W. Wark, H.J. Lee, R.M. Corn, *Anal. Chem.* **77**, 3904 (2005)
- 9 J. Homola, I. Koudela, S.S. Yee, *Sens. Actuators B* **54**, 16 (1999)
- 10 Most of the details for the temperature model can be found in H.-P. Chiang, P.T. Leung, W.S. Tse, *Solid State Commun.* **101**, 45 (1997)
- 11 G.G. Nenninger, P. Tobiska, J. Homola, S.S. Yee, *Sens. Actuators B* **74**, 145 (2001)